Industrial Chemistry Publication Series
Teknillisen kemian julkaisusarja
Espoo 2003 No. 15

KINETIC STUDIES ON THE ETHERIFICATION OF C_5-ALKENES TO FUEL ETHER TAME

Päivi Pääkkönen

Dissertation for the degree of Doctor of Science in Technology to be presented with due permission of the Department of Chemical Technology for public examination and debate in Auditorium Ke 2 (Komppa Auditorium) at Helsinki University of Technology (Espoo, Finland) on the 9th of May, 2003, at 12 o'clock noon.

Helsinki University of Technology
Department of Chemical Technology
Laboratory of Industrial Chemistry

Teknillinen korkeakoulu
Kemian tekniikan osasto
Teknillisen kemian laboratorio

Distribution:
Helsinki University of Technology
Laboratory of Industrial Chemistry
P. O. Box 6100
FIN-02015 HUT
Fax. +358-9-451 2622
E-Mail: paakkonen@polte.hut.fi

ISBN 951-22-6431-5
ISSN 1235-6840

Otamedia Oy
Espoo 2003

Abstract

Tertiary ethers are formed in reactions between alcohols and alkenes and are used in reformulated gasoline as octane-enhancing agents. By blending ethers into the gasoline pool, less ground-level ozone is formed and combustion of the gasoline is more efficient as a result of the oxygen boost.

The main goal of this research was to study the synthesis of TAME (*tert*-amyl methyl ether, 2-methoxy-2-methylbutane) and to formulate a kinetic model as precise as possible for process design purposes. The reaction rate was studied as a function of temperature and the reagents feed molar ratio with conventional ion-exchange resin beads and a novel fibrous ion-exchange catalyst. Kinetic modelling favoured the Langmuir-Hinshelwood type model, derived from a dual-site mechanism for the etherification. The influence of the acid capacity of the catalysts on the reaction rate was found to be second order. These results suggest that the etherification reactions occur via a dual-site mechanism.

Comparison of the values of the kinetic parameters obtained with a fibre catalyst and with a bead catalyst indicated that diffusion limitations are associated with the latter. Therefore, mass transfer of the reacting components inside the pores of the cationic ion-exchange resin bead was estimated in terms of the effectiveness factors calculated from experiments with different resin bead sizes. It was concluded that mass transfer has to be taken into account when applying the kinetic model, which was derived for resin beads as the catalyst.

High temperatures and high alcohol concentrations favoured the formation of the dialkyl ethers (dehydration) as a side reaction. When the reaction was maintained in a kinetic regime, it was highly selective for *tert*-etherification, since the rate of *tert*-etherification was 140 to 270 times that of dehydration. The experimental results were best described with a model in which one alcohol molecule is adsorbed and the other reacts from the liquid phase. The activation energy was determined to be 102.6 kJ/mol for methanol dehydration to yield DME.

The ranges of validity of the other complete kinetic models proposed for the synthesis of TAME in the literature were evaluated by simulating the experimental conditions and by comparing the adequacy of the models in predicting the experimental composition

changes and the composition at reaction equilibrium. Activity-based models were found to predict our experimental results better under a wider range of conditions than concentration-based models.

Preface

The work for this thesis was carried out at Helsinki University of Technology in the Laboratory of Industrial Chemistry between October 1995 and December 1997 and continued between January 2001 and October 2002. Financial support from the Technology Development Centre of Finland, Fortum Oil & Gas Ltd., and the Academy of Finland through the Graduate School in Chemical Engineering (GSCE) is gratefully acknowledged.

I am especially grateful to Professor Outi Krause for her continuous support, encouragement, and valuable advice during the course of my work. I also thank my co-authors, Dr. Liisa Rihko-Struckmann and Dr. Juha Linnekoski, for many fruitful scientific conversations and for their pioneering work with tertiary ethers at HUT, which made my work possible. Many thanks to my colleagues in the laboratory for creating a pleasant atmosphere and supportive environment for research work. Special thanks to Petri Latostenmaa, Jani Porkka, Riikka Puurunen and Jaakko Ruokomäki for carrying out some of the experiments.

Finally, many thanks to my family, relatives and friends for their support during my many years of study. I also wish to express my sincerest gratitude to Dr. Maria Muhonen for keeping up my spirit. This thesis is dedicated to my father, who has been the strenght, and to my mother, who has been the stability in my life.

Espoo, April 2003

Päivi Pääkkönen

LIST OF PAPERS

This thesis is based on the following papers (Appendices I-VI), which are referred to in the summary by their Roman numerals.

I. L.K. Rihko, P.K. Kiviranta-Pääkkönen, A.O.I. Krause, Kinetic Model for the Etherification of Isoamylenes with Methanol, *Ind. Eng. Chem. Res.* **36** (1997) 614-621.

II. P. Kiviranta-Pääkkönen, A.O.I. Krause, Simultaneous Isomerisation and Etherification of Isoamylenes with Methanol, *Chem. Eng. Technol.* **26** (2003) 479-489.

III. P.K. Pääkkönen, A.O.I. Krause, Diffusion and Chemical Reaction in Isoamylene Etherification within a Cation Exchange Resin, *Appl. Catal. A: General* (2003) in press.

IV. P.K. Kiviranta-Pääkkönen, L.K. Struckmann, J.A. Linnekoski, A.O.I. Krause, Dehydration of the Alcohol in the Etherification of Isoamylenes with Methanol and Ethanol, *Ind. Eng. Chem. Res.* **37** (1998) 18-24.

V. P. Kiviranta-Pääkkönen, L. Struckmann, A.O.I. Krause, Comparison of the Various Kinetic Models of TAME Formation by Simulation and Parameter Estimation, *Chem. Eng. Technol.* **21** (1998) 321-326.

VI. P.K. Pääkkönen, A.O.I. Krause, Comparative Study of TAME synthesis on Ion-exchange Resin Beads and a Fibrous Ion-exchange Catalyst, *React. Funct. Polym.* (2003) in press.

Päivi Pääkkönen's contribution to the appended papers:

I The author made the research plan together with the co-authors and she carried out the experiments. She participated in the interpretation of the results and preparation of the manuscript.

II,VI The author made the research plan and carried out the experiments. She interpreted the results and prepared the manuscript.

III The author made the research plan and carried out some of the experiments. She interpreted the results and prepared the manuscript.

IV The author made the research plan and carried out most of the experiments. She interpreted the results and wrote the manuscript together with the co-authors.

V The author carried out the simulation studies and interpreted the results. She wrote the manuscript together with the co-authors.

KINETIC STUDIES ON THE ETHERIFICATION OF C_5-ALKENES TO FUEL ETHER TAME

1. INTRODUCTION

1.1 Ethers as gasoline components

Tertiary ethers are used in gasoline as octane-enhancing agents. Besides the increase in octane ratings, other benefits to gasoline quality are obtained by blending oxygenates. As a result of the oxygen boost, the amounts of toxic carbon monoxide (CO) and hydrocarbons (HC) are reduced in the exhaust gas [1]. Although the oxygen benefit could be obtained from alcohols, tertiary ethers are a better choice because they have lower vapour pressures (Table 1). Ethers are less soluble in water than alcohols, and the solubility in water decreases for heavier ethers. The decrease in the amount of alkenes in the gasoline makes it less volatile and thus ground-level ozone formation is reduced. By blending tertiary ethers with gasoline the amounts of harmful aromatic compounds in gasoline can also be reduced [2].

Table 1. Typical blending properties of alcohols, ethers and alkenes [3-8]

	Average octane $\frac{RON+MON}{2}$	Oxygen content wt-%	Solubility in water wt-%	Blending Rvp bar	Atmospheric reactivity*
Methanol	120 [3]	50 [3]	Soluble [7]	4.1 [3]	1.0 [3]
Ethanol	115 [3]	35 [3]	Soluble [7]	1.2 [3]	3.4 [3]
MTBE	110 [3]	18 [3]	4.3 [4]	0.6 [3]	2.6 [3]
ETBE	111 [3]	16 [3]	1.2 [4]	0.3 [3]	8.1 [3]
TAME	106 [3]	16 [3]	1.2 [4]	0.1 [3]	7.9 [3]
Isobutene	90 [5]	0	0.03 [8]	4.6 [3]	55.0 [3]
2M1B	88 [6]	0	Partly soluble [7]	1.3 [3]	70.0 [3]
2M2B	91 [6]	0	Partly soluble [7]	1.0 [3]	85.0 [3]

* Hydroxyl reaction rate coefficient: 10^{12} cm^3 $molecule^{-1}s^{-1}$

With increasingly strict legislation the need for tertiary ethers has grown steadily and turned the focus from MTBE (methyl *tert*-butyl ether, 2-methoxy-2-methylpropane) towards heavier ethers like TAME (*tert*-amyl methyl ether, 2-methoxy-2-methylbutane), since the supply of isobutene is limited and the future of MTBE is uncertain due to California banning it from the beginning of 2004. A major reason for the growing interest in the ethanol-based tertiary ethers ETBE (ethyl *tert*-butyl ether, 2-ethoxy-2-methylpropane) and TAEE (*tert*-amyl ethyl ether, 2-ethoxy-2-methylbutane) is that ethanol can be produced by fermentation from renewable resources [9]. The production figures for tertiary ethers in 1998 are presented in Table 2.

Table 2. The production capacities for tertiary ethers in 1998 [9]

	Global production capacity m^3/a	Capacity under construction m^3/a
MTBE	30 350 000	3 020 000
ETBE	5 281 000	1 219 000
TAME	2 669 000	928 000

In Europe, there were 37 production plants for ether oxygenates (MTBE, ETBE and TAME) in December 2000, the majority (29) of which produced MTBE. The production capacity of the plants ranged from 15,000 tonnes to over 600,000 tonnes per year and the total European ether capacity was estimated to be 3,991,000 tonnes per year [10].

1.2 Production of ethers

Ether synthesis is typically carried out under pressure in the liquid phase over a strongly acidic macroporous ion-exchange resin as the catalyst. The conventional ion-exchange resins are copolymers of divinylbenzene (DVB) and styrene, sulfonic acid being the active site (Bröndstedt acidity). Lewis acidity (free electron pairs of oxygen) of the catalyst has also been proposed [11]. A tertiary ether is formed from a reaction between an alcohol and an alkene containing a double-bonded tertiary carbon atom:

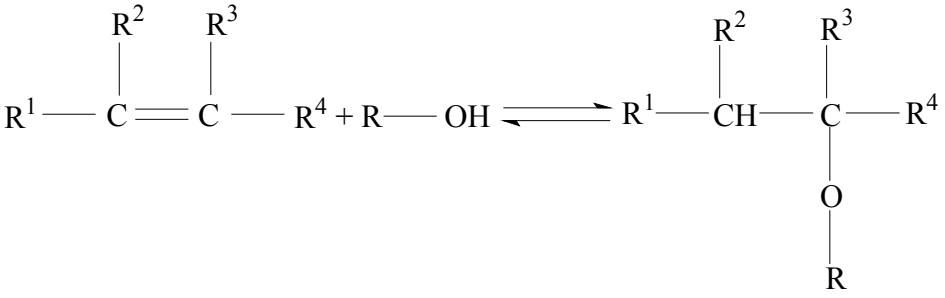

(1)

The ether synthesis reactions are governed by thermodynamic equilibrium and are shifted towards ether formation at low temperatures. The reaction kinetics, on the other hand, are favorable at higher temperatures. The reactor design is therefore a compromise between thermodynamic and kinetic considerations. Sufficiently low temperature also diminishes the side reactions and prolongs the life of the catalyst [3].

An alcohol/alkene ratio greater than 1 increases the conversion and suppresses the dimerisation and polymerisation of the alkenes but simultaneously increases the cost of recovery and recycling of the unreacted alcohol. The formation of dialkyl ethers from the dehydration reaction of alcohols are also favoured by high alcohol concentrations. Therefore the optimum alcohol/alkene ratio is near to the stoichiometric one [12]. For

example, at a molar methanol excess as low as 10 %, the selectivity for MTBE is practically 100 % [13].

In commercial applications the first reactor, where most of the conversion takes place, is often a fixed bed adiabatic reactor. This choice, leading to an increasing temperature along the reactor axis, is not optimal. In fact, the best compromise between the kinetics and thermodynamics is achieved by higher temperatures in the inlet zone, to allow high reaction rates, and lower temperatures in the outlet zone, to approach equilibrium at higher conversions. Reactive distillation, which combines reaction and distillation in a single operation, has found application only in the second stage of the operation, where heat effects are negligible. The difficulty controlling the heat released by the exothermic reactions may cause substantial vaporization in the middle section of the column [14]. Another challenge with reactive distillation is to maintain an adequate alcohol/alkene ratio in the liquid phase in contact with the catalyst [4]. This is because the reactant ratios are a function of conversion and azeotrope formation, the operating pressure affects the relative volatility, chemical equilibrium and reaction rate, and the reflux ratio impacts both separation and conversion [15].

In Figures 1 and 2 two different process schemes are presented. They employ reaction and distillation separately, thus avoiding the problems related to reactive distillation.

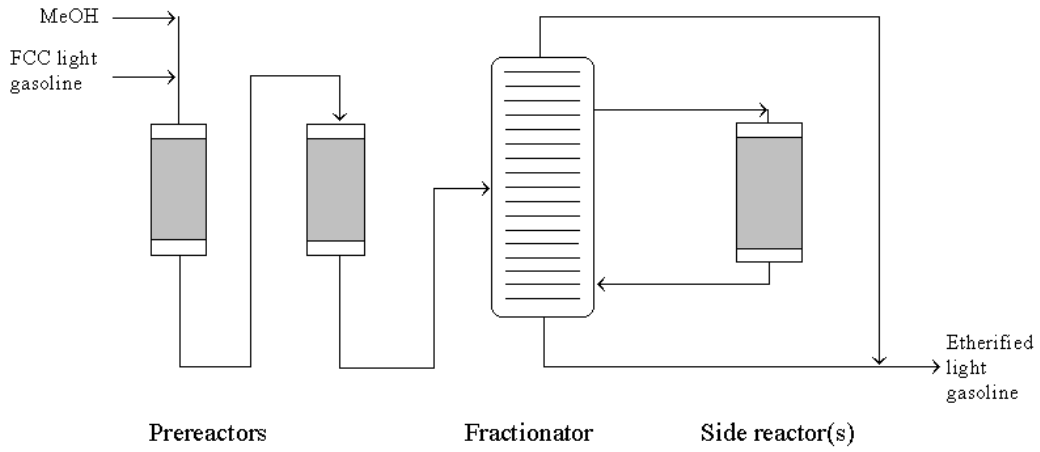

Figure 1. The NexTAME process [16]

In the NexTAME process the temperatures of the prereactors are decreased successively. This maximizes the overall conversion, being about 65 % for C_5-alkenes, 35 % for C_6-alkenes and 25 % for C_7-alkenes. The key feature is the side reactor configuration. The side-stream draw-off is taken from the fractionator column above the feed point and adjusted to the reaction temperature with a heat exchanger. The side reactor product is fed back to the fractionator below the feed point. Before feedback the product is heated, thus enabling optimisation of the fractionator concentration profiles. Methanol cannot leave the fractionator from the bottom or the top, so it concentrates in the side loop together with reactive alkenes. Therefore, a separate alcohol recovery section is not needed [16].

The Phillips process uses a similar approach to NexTAME. In this process the catalyst is located in the reflux loop of the fractionator, so that the alcohol/alkene ratio is maintained at the optimum throughout the entire catalyst bed. This configuration also allows the catalyst to be operated at the optimum temperature without affecting the distillation operation. In the Phillips process a separate alcohol recovery section is needed, however [4].

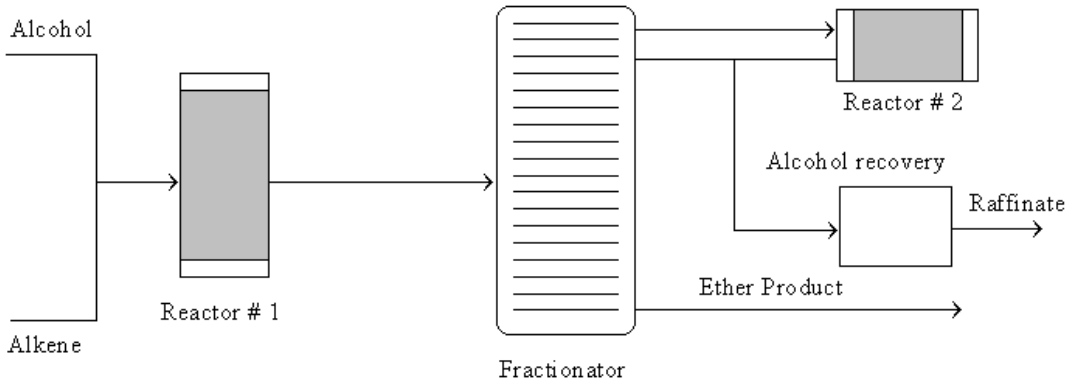

Figure 2. The Phillips High-Conversion Etherification Process [4]

1.3 The scope of this study

Precise kinetic models are valuable in process design because they are the basis for both feasible and intrinsically cleaner processes. Kinetic models based on reasonable mechanistic knowledge or assumptions are generally preferred over empirical ones because the scale-up from laboratory to industrial process is on safer ground when a mechanistic model is available. For the synthesis of TAME a proper kinetic model with a correctly predicted reaction equilibrium is essential in the design of the etherification process. Moreover, the model should cover a wide range of conditions because in novel etherification processes the etherification conversions can be maximised by side reactor configuration or by reactive distillation. Under these conditions, the methanol/isoamylene ratio can differ greatly from the stoichiometric value [4,16].

So far, the majority of kinetic models published for tertiary ethers deal only with the main reactions. However, it is also important to investigate the formation of by-products because of the specifications that are defined within an oil refinery both for the gasoline

product and for the intermediates. Etherification reactions are exothermic and possible hot spots resulting from uneven cooling may lead to unwanted side reactions. Typical side reactions are the dehydration of the alcohol to yield dialkyl ether and water, hydration of isoamylenes to yield a tertiary alcohol, and dimerisation of isoamylenes [4].

The principle aim of this study was to develop a kinetic model for the synthesis of TAME, as precise as possible within the limits of the analytical accuracy [I-III], for reactor design purposes. The second goal was to study the side reactions [IV]. In paper V other kinetic models for the synthesis of TAME presented in the open literature were evaluated against our experimental data. Further mechanistic evidence was sought by studying different catalysts in TAME synthesis [VI].

2. EXPERIMENTAL

2.1 Catalysts

Commercial macroporous cation ion-exchange resin beads in hydrogen-form (Amberlyst 16 [I-VI]; Amberlyst 35 [VI]; XE586 [VI] from Rohm & Haas) and ion-exchange fibre (Smopex-101 [VI] from Smoptech Ltd.) were used as the catalysts in the kinetic experiments. Before the experiments, the catalysts were washed with methanol (bead catalysts [I-VI]) or ethanol (A16 [IV] and fibre catalyst [VI]). The bead catalysts were stored in methanol or ethanol (A16 [IV]), but the fibre catalyst was dried in an oven (100°C) to remove moisture and other impurities and stored dry in a desiccator [VI]. The properties of the catalysts are summarised in Table 3.

Table 3. Properties of the catalysts studied.

	A16	**A35**	**XE586**	**SMOPEX-101**
Crosslink level	medium	high	medium	
Exchange capacity (mmol/g)	5.0	5.2	1.3	3.4
Surface area (m^2/g)	35	45-50	75	
Average pore diameter (nm)	20	25-30	20	
Porosity	0.25	0.35	0.35	
Particle size (mm) ^{m} = mean size ^{s} = swollen diameter	0.7^{m} [I, IV, V] 0.3-0.6 [II] fractions [III]: **1**) $0.50\text{-}0.59^{s}$ **2**) $0.59\text{-}0.71^{s}$ **3**) $>0.71^{s}$ 0.38-0.45 [VI]	0.15-0.25 [VI]	0.7^{m}[VI]	powder [VI]

2.2 Chemicals

The following reagents were used in the experiments: p.a. grade 2M1B (Aldrich, 99.8 wt-%) [I,II,VI]; redistilled 2M2B (Aldrich, 99 wt-%) [VI]; mixture of isoamylenes (Fluka Chemika, 2M2B, technical grade) with a composition of 2M2B 91.5-93.2 wt-% and 2M1B 6.8-8.5 wt-% [I,III-IV,VI]; p.a. grade MeOH (Merck [I]/Riedel-de Haën [II-IV,VI], >99.8 wt-%); p.a. grade isopentane (Fluka Chemika) [II,IV,VI] or p.a. grade isooctane (Fluka Chemika) [II] were used as inert solvents. The ether, TAME, was supplied by Yarsintez, Russia [I] or by Fortum Gas & Oil Ltd. [II-IV,VI] and the purity was >98.5 wt-% or >98.0-98.5 wt-%, respectively.

2.3 Equipment

All the experiments were carried out in the liquid phase by keeping the pressure above 0.7 MPa. The temperatures used were: from 333 to 353 K [I], 333 K [II], from 323 to 353 K [III], from 323 to 363 K [IV], and from 323 to 353 K [VI]. Two stirred tank reactors in batch and continuous mode were used in the studies.

2.3.1 Batch reactor

The kinetic experiments [I,II,VI] were carried out in an 80 cm^3 stainless steel vessel, where the reaction mixture was stirred magnetically and the temperature was controlled within ± 0.25 K by immersing the reactor in a thermostated water bath. On the reactor walls there were vertical mixing baffles in order to guarantee complete mixing. The catalyst (A16, 0.2-1.8 g [I-II]) was placed in the metal gauze basket or used in the reactor as slurry (SMOPEX-101, 0.3-0.7 g [VI]). The samples were taken manually via an ice-cooled sample valve at the top of the reactor.

2.3.2 Continuous stirred tank reactor

In studies III-IV and VI the steady state reaction rates were measured in a continuous stirred tank reactor of volume 55.6 cm^3 (stainless steel), where the reaction mixture was magnetically stirred. The catalysts were placed in the metal gauze basket (A16, 0.2-0.3 g [III], 0.2-2.3 g [IV] or 0.3 g [VI], and XE586, 0.3 g [VI]) or used in the reactor as slurry (SMOPEX-101, 0.7 g and A35, 0.3 g [VI]). The pulse-free flow rate (5-82 g/h) of the feed was controlled by a liquid mass flow controller. A Mettler PM 6000 balance was used to measure the actual flow at the outlet of the reactor system. The composition of the feed and the reactor effluent were analyzed on-line with a gas chromatograph using an automated liquid sampling valve.

2.4 Analysis

The products were analysed with a Hewlett-Packard gas chromatograph 5890 Series II, equipped with a flame ionisation detector using a HP 3396A integrator. The compounds were separated in a glass capillary column DB-1 (length 60 m, film thickness 1.0 μm, column diameter 0.254 mm; J & W Scientific). The response factors of the components were determined with calibration solutions in order to obtain quantitative results. The reproducibility of the analysis was ± 3 % (batch reactor experiments) and ± 1 % (CSTR experiments).

2.5 Calculations

In this study, all reaction rates were calculated on the basis of the weight of the *dried* catalyst. The calculation of the initial rates (batch reactor experiments) was made by regression from the slopes of the straight lines of the initial experimental ether and alkene amounts (mol) as a function of contact time (time × catalyst weight) [I,II,VI]. The steady

state reaction rates of the CSTR experiments were calculated on the basis of the catalyst weight [III, IV, VI],

$$r_{obs} = \frac{(F_{T,out} - F_{T,in})}{W_{cat}} = \frac{(w_{T,out} - w_{T,in})\,\dot{m}_{tot}}{M_T W_{cat}} \qquad (2)$$

or by taking into account the number of sulfonic acid groups according to a first order dependency [III, VI] and a second order dependency [VI]:

$$r_{obs} = \frac{(F_{T,out} - F_{T,in})}{W_{cat}(H^+)} = \frac{(w_{T,out} - w_{T,in})\,\dot{m}_{tot}}{M_T W_{cat}(H^+)} \qquad (3)$$

$$r_{obs} = \frac{(F_{T,out} - F_{T,in})}{W_{cat}(H^+)^2} = \frac{(w_{T,out} - w_{T,in})\,\dot{m}_{tot}}{M_T W_{cat}(H^+)^2} \qquad (4)$$

Conversions and fractional conversions were calculated on a molar basis.

The nonideality of the reaction mixtures was taken into account by applying activities instead of concentrations in the kinetic modelling. The activities were calculated from the activity coefficients and the molar fractions of the components:

$$a_i = \gamma_i x_i \qquad (5)$$

The activity coefficients were estimated with the UNIQUAC method [17] in paper I, with the UNIFAC method [18] in papers IV-V and with the Wilson method [19] in papers II, III, VI.

3. MACROKINETIC MODEL WITH AMBERLYST 16

3.1 Kinetic experiments with Amberlyst 16

In the first part of this thesis [I] the effect of the reagents initial molar ratio (MeOH/IA=0.2-2.0) and temperature (333-353 K) on the synthesis of TAME was studied. Simultaneous isomerisation and etherification reaction rates were studied with an equimolar mixture of pure 2M1B and MeOH in the feed at different temperatures. In the second part of the thesis [II] simultaneous isomerisation and etherification at 333 K was studied in more depth by changing the initial molar ratio of pure 2M1B and MeOH. Solvents were used in some of the experiments. The calculated initial rates of etherification are presented in Table 4.

Table 4. Initial rates of etherication (mmol/g*h) under different conditions

Feed ratio	333 K		338 K		343 K		353 K	
MeOH/ alkene	IA	2M1B	IA	2M1B	IA	2M1B	IA	2M1B
0.2	43	149-153	64		125		329	
0.5-0.6	45	183	80		144		299	
0.9-1.0	44	114	80	157-160	116	352	213	516-527
1.2-1.3	29	121	46		74		155	
2.0	30		44		70		165	
4.1		86						

The table shows that the initial reaction rate to TAME decreases with increasing MeOH/alkene molar ratio in the feed. The initial reaction rate from pure 2M1B is two to three times faster than from the equilibrium mixture of the two isoamylenes. The ratio of the etherification and isomerisation rates is 2-3 until the lowest initial MeOH/2M1B molar ratio of 0.2, when the isomerisation rate increases significantly. At a MeOH/2M1B molar ratio of 0.2 the isomerisation reaction rate is twice as high as the etherification reaction rate (see Figure 3, at x_{1b}=0.8).

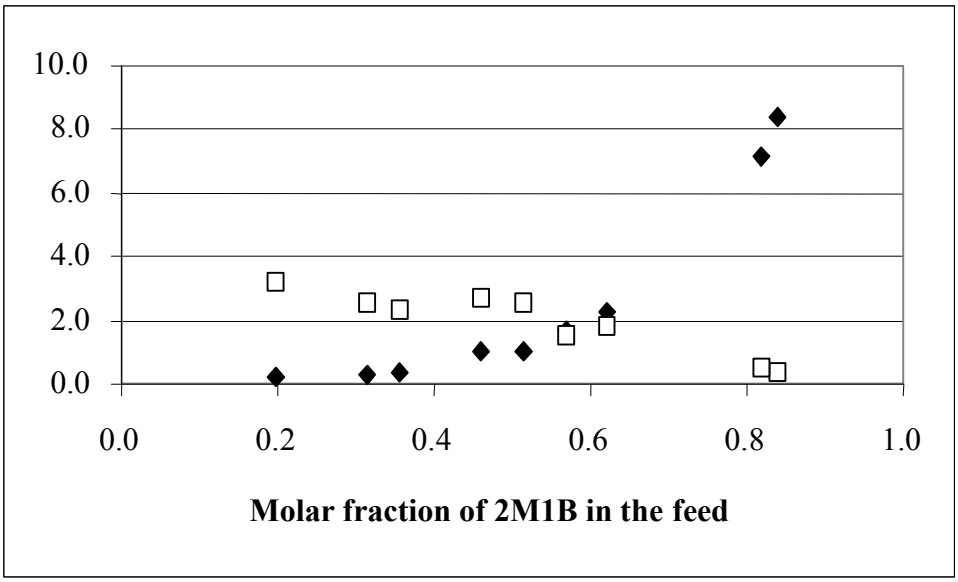

Figure 3. (◆) Normalised rate of isomerisation (initial isomerisation rate/initial isomerisation rate under stoichiometric conditions) and (□) ratio of the etherification and isomerisation rates as a function of the amount of 2M1B in the feed

Figure 3 also shows how the relative isomerisation rate (ratio of rates = isomerisation rate/isomerisation rate under stoichiometric conditions) increases exponentially with the molar fraction of 2M1B in the feed reaction mixture. The ratio of the rates varies between 0.2 at x_{1b}=0.2 and 8 at x_{1b}=0.8. This result could indicate that migration of the alkenes

inside the catalyst pores to the active site of the catalyst depends exponentially on the amount of the alkene and is less hindered when the amount of the alcohol in the reaction mixture is small. The acidity of the catalyst might also become greater when the sulfonic acid groups are less solvated by methanol.

3.2 Kinetic modelling

In the first part of this thesis [I] kinetic modelling was carried out separately for each batch reactor experiment. Three kinetic models based on different mechanistic assumptions were compared:

A) homogeneous

B) adsorption of the alcohol and the ether

C) adsorption of all components

The kinetic equations were written in terms of activities because of the non-ideality of the liquid phase, as it was a mixture of polar and non-polar substances.

From the results of the regression analysis, it could be concluded that mechanism A is the least probable. The weighted sum of residual squares was the highest for this mechanism. The results of the regression analysis further indicated that both mechanisms B and C could possibly describe the experimental data. However, in the parameter estimation for mechanism C, the convergence was not satisfactory in the optimisation under all conditions. This was observed especially in experiments where the molar ratio of methanol/isoamylene was 0.2. In this respect, the experimental results were best described by kinetic equations, which were based on the mechanism (B) where the alcohol and the ether adsorbed on the catalyst surface and the isoamylenes reacted from the liquid phase. The unsatisfactory convergence of mechanism C was probably a result

of the numerical manipulations (equations 13-15/[I]), which had to be carried out because of the lack of adsorption equilibrium data. However, the values of the rate parameters obtained (mechanism B) were not constant under different conditions, but were highly dependent on the molar feed ratio of the reagents (Table 3/[I]). In addition, the model could not describe the reaction rates when the amount of methanol was low (less than 5 wt-%) (Figure 2/[II]). The other more fundamental weakness of the model was that the isomerisation reaction was assumed to happen noncatalytically. To improve the model, we decided to study the isomerisation reaction with more experiments and further kinetic modelling.

Therefore, in the second part of the thesis several basic models based on different mechanistic assumptions (Table 2/[II]) were tested against the data set from batch reactor experiments with Amberlyst 16 as the catalyst (359 samples). The data points from the two extreme experiments where the initial methanol/2M1B molar ratio was 0.2 were excluded from this regression analysis. In deriving all the equations it was assumed that the surface reaction is the rate determining step and that the alcohol adsorbs most [20]. Basic models based on two or three active sites participating in the reaction gave the best fits.

Because accurate adsorption equilibrium measurements had been published [21] after paper I it was possible, without estimating the adsorption equilibrium constants, to compare the residual sum of squares of the different *precise* correlations (Table 4/[II]). These correlations therefore had the same number (6) of estimated parameters, *i.e.* only the reaction rate parameters (k_1, k_3 and k_5) and their corresponding activation energies. The data points from the two experiments carried out with an initial methanol/2M1B molar ratio of 0.2 were included in this further analysis (total 375 samples). It was

concluded that, although the best fit was obtained with a model for which the mechanism was based on three active sites (Bröndstedt and Lewis acidity), the second best model of basic Langmuir-Hinshelwood type was considered to be more likely from a purely mechanistic point of view [22]. An empirical correction factor describing the acceleration of isomerisation kinetics (see Figure 3) was inserted into the kinetic equations, which resulted in further improvement of the fit and even more precise values of the model parameters. The model is presented in equations (6) and (7) and its parameters are presented in Table 5.

$$r_{ETHER} = \frac{k_1 \frac{K_{1b}}{K_M} a_M a_{1b} \left(1 - \frac{a_T}{K_1 a_M a_{1b}}\right) + k_3 \frac{K_{2b}}{K_M} a_M a_{2b} \left(1 - \frac{a_T}{K_2 a_M a_{2b}}\right)}{\left(\frac{K_T}{K_M} a_T + a_M + \frac{K_{1b}}{K_M} a_{1b} + \frac{K_{2b}}{K_M} a_{2b}\right)^2} \quad (6)$$

$$r_{ISOM} = \frac{k_5 \frac{K_{1b}}{K_M} a_{1b} \left(1 - \frac{a_{2b}}{K_3 a_{1b}}\right) 0.0006 \exp(6.148 * x_{1b})}{\left(\frac{K_T}{K_M} a_T + a_M + \frac{K_{1b}}{K_M} a_{1b} + \frac{K_{2b}}{K_M} a_{2b}\right)} \quad (7)$$

Table 5. Values of the parameters of the proposed model

Parameter	k_i (at 333 K) ± SE mol kg^{-1} s^{-1}	E_{act} ± SE J mol^{-1}
k_1	0.9786 ± 0.0194	101978 ± 1650
k_3	0.4220 ± 0.0042	101087 ± 853
k_5	61.66 ± 2.19	97210 ± 4539
K_1	[19]	$=\exp(-8.74435 + 4142.069/T)$
K_2	[19]	$=\exp(-8.24371 + 3219.118/T)$
K_3		$=K_1/K_2$
K_{1b}/K_M	[21]	$= \exp(-13.0304 + 3171.451/T)$
K_{2b}/K_M	[21]	$= \exp(-9.22212 + 1852.525/T)$
K_T/K_M	[21]	$= \exp(-7.32796 + 1050.648/T)$

A Langmuir-Hinshelwood type model has also been proposed by Pavlova *et al*. [23] and Oost and Hoffmann [24] for the synthesis of TAME. Pavlova *et al.* obtained an activation energy of 63.1 kJ/mol for the etherification of 2M1B, 78.3 kJ/mol for the etherification of 2M2B and 76.6 kJ/mol for the isomerisation of 2M1B to 2M2B from batch reactor experiments with polyethene-based KIF-2 used as the catalyst. Oost and Hoffmann combined the two isoamylenes in their kinetic analysis of continuous recycle reactor experiments with Lewatit SPC 118/108 used as the catalyst and obtained an average activation energy of 89.5 kJ/mol for the etherification and 90.3 kJ/mol for the isomerisation. The activation energies in Table 5 are at a much higher level. This must be a consequence of the form of the kinetic equations, mainly of the equation proposed for isomerisation (equation 7). If the empirical equation describing the acceleration of isomerisation kinetics is not included in the model, the obtained activation energies are: 84.6 kJ/mol for the etherification of 2M1B, 103 kJ/mol for the etherification of 2M2B and 70.7 kJ/mol for the isomerisation of 2M1B to 2M2B (Table 7/[II]).

However, simulation studies revealed (see Figure 4) that the proposed model could not predict the experimental rates when the amount of the alcohol in the mixture was small (less than 5 wt-% or 10 mol-%). The predicted reaction rate was again slower than the experimental one. The other model based on three active sites, on the other hand, predicted higher reaction rates than experimentally measured. It is difficult to interpret whether a transition in the reaction mechanism takes place under low alcohol concentrations or if the high reaction rate is a consequence of less hindered diffusion of alkenes to the active site of the catalyst. The acidity of the catalyst might also become higher because the protons are less solvated by the alcohol when the amount of the

alcohol in the reaction mixture gets smaller. Anyhow, whatever the reason for the accelerating reaction rate, the validity of the proposed model is restricted to the presence of alcohol in amounts *greater* than 5 wt-% or 10 mol-%.

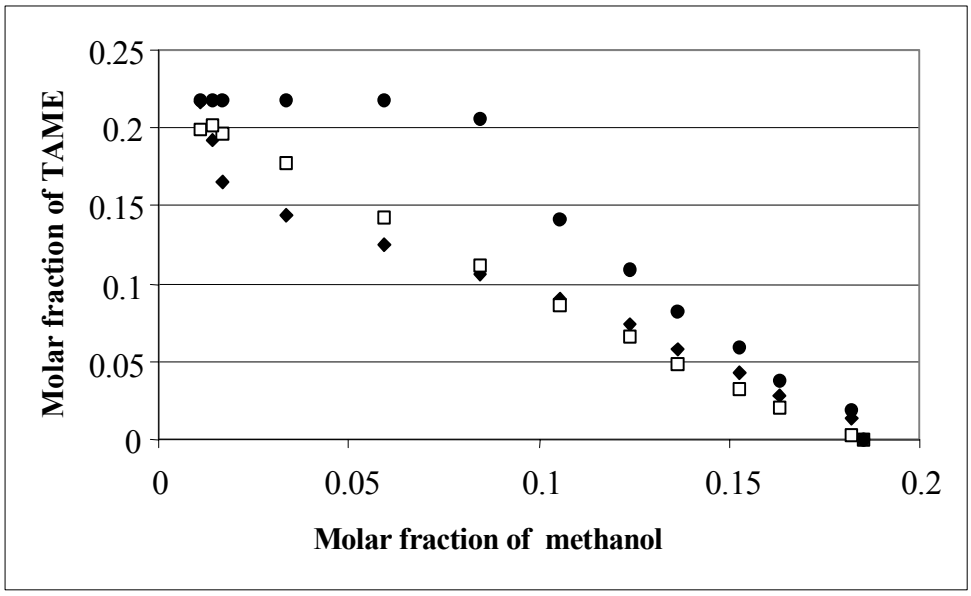

Figure 4. Simulated and experimental molar fractions of TAME at 343 K with a methanol/isoamylenes feed ratio of 0.2. Predictions with the proposed model (◆) and with the Lewis-Bröndstedt model [11] (●); experimental points (□).

4. MASS TRANSFER

Because unsieved catalyst was used in most of the kinetic experiments with Amberlyst 16 [I], there was no assurance that our kinetic results were truly intrinsic, even though basic tests had been carried out earlier [25]. Another intriguing observation was that when the kinetic modelling was carried out separately for each batch reactor experiment, the values of the estimated rate parameters were highly dependent on the feed molar ratio of the

reagents, regardless of the applied kinetic model (Eley-Rideal type: Table 3/[I] and basic Langmuir-Hinshelwood type: Figure 4/[III]). Therefore, mass transfer was studied in the third part of this thesis [III]. The formation rates of TAME were measured with different Amberlyst 16 particle sizes under different experimental conditions. The effect of catalyst swelling was studied with several mixtures of reagents (MeOH and IA) and product (TAME) on Amberlyst 16 in order to get an estimate of the "true" radius of the catalyst particles. Qualitatively it was concluded that the diffusion rate of the reagents in the pores of the cation exchange resin had a significant influence on the observed reaction rate (Figures 1a)-c)/[III]).

For quantitative conclusions, the effective radius was calculated from the swelling experiments and the effective diffusion coefficients were estimated with the Scheibel method [26], corrected to liquid phase activities with the Vignes equation [27]. Because the studied reaction forms a ternary system (MeOH, isoamylene, TAME), the equation by Kooijman and Taylor [28] was further applied to estimate the diffusion coefficients in the multicomponent mixture. The observed rate coefficients were calculated with the kinetic model of Langmuir-Hinshelwood type (equation 6).

The Thiele modulus was calculated according to method by Aris [29] for a second-order Langmuir-Hinshelwood kinetics and the effectiveness factors were obtained graphically from the generalised curves by Aris [29].

The determined effectiveness factors for rate parameter k_3 were presented in Figure 3/[III]. The estimated effectiveness factor (0.5-1.0) decreased with increasing particle size and increasing temperature. For nonstoichiometric feed ratios of the reagents the value of the effectiveness factor decreased more when methanol was fed in excess.

The batch reactor results of the earlier studies [I-II] were recalculated by dividing the rate constants of the TAME synthesis by the effectiveness factors estimated from the experiments of the third study [III]. These calculations demonstrated that when modifying the rate constants of the *basic* Langmuir-Hinshelwood type kinetic model (without the empirical equation of isomerisation kinetics and relative adsorption equilibrium constants) in this way, the R-squared values of the regression analysis against temperature increased (better fit for Arrhenius-type dependency). The activation energies also increased by about 9 kJ/mol to 82 kJ/mol for the etherification of 2M1B and to 95 kJ/mol for the etherification of 2M2B, values which were more satisfactorily within an intrinsic range (compared to the values in Table 5/[III] and Table 3/[II]).

In a recent study by Jin *et al*. [30] the kinetics of TAME synthesis in an internal recycle *gradient-less* reactor with an ion-exchange resin, NKC-9, as catalyst has been studied. The authors found that the Langmuir-Hinshelwood type model was particularly appropriate and derived activation energies of 96.78 kJ/mol for the etherification of 2M1B and 102.4 kJ/mol for the etherification of 2M2B. Our observed activation energies (100-108 kJ/mol, Table 6/[III]) for the precise Langmuir-Hinshelwood type model are thus in satisfactory agreement with the latter value. The activation energies presented in Table 5 (p. 22) are also quite satisfactorily within the intrinsic range, since the mass transfer effect of the alkene (2M1B) has been kind of taken into account in the proposed empirical equation for isomerisation kinetics in the form of exponential acceleration of the isomerisation rate. Even though the obtained activation energies do not indicate strong diffusion limitations, the calculated effectiveness factors (0.5-1.0) in paper III suggest that mass transfer effects also have to be taken into account in TAME synthesis with resin

beads as the catalyst, even though the reaction rate is an order of magnitude slower than that of MTBE synthesis [31].

5. SIDE REACTIONS

Commercially, TAME synthesis is carried out by feeding excess alcohol into the reactor in order to maximize conversion of the alkenes. In the NexTAME process there is a significant excess of the alcohol in the side-reactor loop. It was therefore of interest to study the dehydration reaction of the alcohol in detail and to also formulate the reaction kinetics. To this end, the effect of temperature and reagent concentration on the formation rates of TAME and DME, as well as TAEE and DEE, were measured in a continuous stirred tank reactor, using a commercial ion-exchange resin (Amberlyst 16) as the catalyst in paper IV.

The basic DME and DEE experiments were carried out both with undiluted methanol and ethanol, and with methanol and ethanol diluted with isopentane so that the molar fraction of alcohol in the mixture was 0.2. The temperature range was 323-363 K.

The formation rate of the dehydration products from plain alcohols as a function of temperature was presented in Figure 1/[IV]. The results showed that DME and DEE formation was favoured by higher temperatures. Moreover, the reactions were not thermodynamically limited within the range investigated. In Figure 1/[IV] the reaction rates of alcohols cannot be directly compared because of the concentration difference resulting from different mole specific densities.

In order to study alcohol dehydration as a side reaction of the formation of tertiary ethers, runs were carried out in the conditions where the amount of isoamylenes was kept constant and the molar ratio of alcohol to isoamylenes was varied from 5 to 20. Isopentane was used as a solvent. The temperature range was 333-353 K. The space time (=amount of catalyst/mass flow rate) was varied from 0.06 to 0.31 h.

The results of varying concentration at a temperature of 353 K were presented in Figure 2/[IV]. A clear difference was seen between the dehydration rates of methanol and ethanol, the rate of methanol dehydration being greater than that of ethanol. At 343 K the same difference was observed, but at 333 K the dehydration rates were the same.

When the reaction was maintained in a kinetic regime, the reaction was highly selective for *tert*-etherification, since the rate of *tert*-etherification was 140 to 270 times that of dehydration. Although no similar experiments were carried out for TAEE, the reaction for *tert*-etherification (TAEE formation) must be highly selective, as the dehydration rate of ethanol was even smaller than the dehydration rate of methanol.

Two types of kinetic models were compared for the dehydration reactions (Table 4/[IV]):

1) single-site reaction of the alcohol

2) dual-site reaction of the alcohol

Linear regression analysis provided statistical support for Model 1. Additional support was based on the plots of the experimental and calculated rates of dehydration. Though there was some experimental fluctuation, the plots showed that the deviation was more severe with Model 2 (Figures 5 and 6/[IV]). Moreover, according to Laidler [32] an Eley-

Rideal type mechanism (Model 1) is expected if the plot of rate vs. concentration reaches an asymptotic maximum value similar to that presented in Figure 2/[IV].

It was assumed that within the experimental range studied the alcohol dehydration was better described with a model where one alcohol molecule is adsorbed and the other reacts from the liquid phase. The difference between the dehydration rates of methanol and ethanol was explained in terms of their differences in polarity. Being the more polar component, methanol has a greater tendency than ethanol to form hydrogen bonds with the sulfonic acid groups, thus dehydrating more vigorously.

6. SIMULATION WITH VARIOUS KINETIC MODELS

The purpose of this study [V] was twofold: to see how other authors have dealt with the complexity of the TAME system, and to test the various kinetic models presented in the open literature against the same experimental batch reactor data, from which the values of our model parameters were partially obtained [I]. The other complete kinetic models proposed for the synthesis of TAME with comparable catalysts are limited to a few publications (see Table 6).

The first model to be tested was the concentration-based model by Hwang and Wu [33]. The authors considered the isoamylenes together, giving one rate parameter and one equilibrium constant for both etherification reactions. Hwang and Wu took into account the nonideality of the liquid phase by applying the UNIFAC method for the calculation of the component activities under equilibrium conditions. In this way, they obtained the

value of the activity-based equilibrium constant, but surprisingly the activity-based equilibrium constant and concentrations of components were combined in the rate equation. The rate expression was based on a pseudo-homogeneous mechanism.

Table 6. Several kinetic models proposed for the synthesis of TAME

Ref.	Feed	Catalyst	Reactor	Temp. °C	Rate Expression for TAME Rate of Isomerisation to 2M2B
[I]	MeOH/IA: 0.2-2.0 MeOH/2M1B: 1.0	A16	Batch	60-80	$r_T = \frac{k_1 a_M a_{1B}(1-\frac{a_T}{K_1 a_M a_{1B}})}{(\frac{K_T}{K_M}a_T + a_M)} + \frac{k_3 a_M a_{2B}(1-\frac{a_T}{K_2 a_M a_{2B}})}{(\frac{K_T}{K_M}a_T + a_M)}$ $r_{2B,isom} = k_5(a_{1B} - \frac{a_{2B}}{K_3})$
[33]	MeOH/IA > 1 C5-cut	A15	Batch PB	40-80	$r_T = k_{13}(C_{IA}C_M - C_T / K_{12})$
[34]	MeOH/2M1B: 1-3 MeOH/2M2B: 1-3	A15	Batch	50-80	$r_T = \sum_{i=1,2} k_{iB}(C_{iB} - C_T / (K_{iB} * x_M^{0.4}))$
[24,38]	MeOH/IA: 0.5-7.9 solvent: n-pentane	Lewatit SPC 118 Lewatit SPC 108	CFRR	50-70	$r_T = k_{1,3}(\frac{a_{1B}}{a_M} - \frac{a_T}{K_1 a_M^2})$ $r_{2B,isom} = k_5(a_{1B} - \frac{a_{2B}}{K_3})$

The model by Piccoli and Lovisi [34] is also a concentration-based model, and the authors pointed out that their model is valid only under conditions where the methanol/isoamylene molar ratio is greater than 1. They studied the two isoamylenes

separately, giving two rate constants and two equilibrium constants. However, they gave no results or conclusions regarding the isomerisation reaction. The kinetic model was based on the ionic mechanism, in which methanol forms a solvated layer around the catalyst site through which the isoamylenes should migrate to adsorb on the site already occupied by methanol. The reaction would then occur by transfer of a H^+ ion to the double bond of the iso-alkene, forming an intermediate carbocation. This surface reaction was assumed to be the rate-controlling step. They calculated the activities of components at equilibrium using the UNIFAC method and further modified the equilibrium constants to depend on the molar fraction of the methanol, which is seen in the form of the rate equation.

Oost and Hoffmann [24] derived their model from the classical Langmuir-Hinshelwood approach assuming that only methanol is adsorbed and that there are no vacant sites present, since the reaction proceeds in the liquid phase. Their kinetic equations are expressed in terms of component activities. They grouped the isoamylenes together as they concluded that the isomerisation reaction is very fast compared to the etherification reaction. They gave one combined rate parameter determining the etherification rate, and values of the equilibrium constants which were obtained from calculations with thermodynamic data [35].

Later, Thiel and Hoffmann [36] proposed that a value of -114.65 kJ/mol for $\Delta_f G$ of TAME, which was calculated from the experimentally determined values of the equilibrium constants by Rihko *et al*. [37], should be used instead of a value of -109.55 kJ/mol obtained from thermodynamic data [35]. So the fourth model to be tested was the kinetic model of Oost and Hoffmann, in which the experimentally determined values for

the equilibrium constants by Rihko *et al*. [37] were applied, as proposed also by Thiel *et al.* [38].

The range of validity of these models was evaluated by simulating our experimental conditions and by comparing the adequacy of the models in predicting the experimental changes in composition as a function of contact time, and composition at reaction equilibrium. The range of validity of the different models according to the simulation studies was summarised in Table 3/[V]. Models based on component activities describe the etherification kinetics and reaction equilibrium better within a wider range of conditions than models based on component concentrations. Both concentration-based homogeneous models describe the kinetics and equilibrium under conditions where methanol is initially in excess. One reason might be that the parameters of the two concentration-based models were obtained from experiments where methanol was initially in excess. The activity-based model by Oost and Hoffmann [24] predicted the experimental changes under a wide range of conditions after revisions to the originally presented values of the equilibrium and isomerisation rate constants had been made. Under conditions of excess methanol the model predicts higher reaction rates than experimentally obtained (Figure 5 b)/[V]). The reason for this could be the diffusion limitations in our experiments as calculated in paper III. Our kinetic experiments were carried out with unsieved catalyst (mean size 0.7 mm) [I], whereas the value of the combined rate parameter for Oost and Hoffmann [24] was obtained from experiments carried out with a particle size of 0.200-0.315 mm.

Our Eley-Rideal type model [I] has been tested independently by Su and Chang [39] in the modelling and simulation of a tubular reactor in the TAME synthesis process with Amberlyst 15 (mean diameter 0.75 mm) as the catalyst. They found out that the simulated

reactor outlet temperatures agreed very well with the operating data and that the predicted temperature profile was reasonably consistent. Moreover, the calculated isoamylene conversions of 63.5% (after the first reactor) and 71.7% (after the second reactor) were very close (within 3% deviation) to those of the performance test.

7. COMPARISON OF CATALYSTS

7.1 Activities of the different catalysts

Up to this point in the study catalysts with constant acid capacity had been used [I-V], meaning that the influence of the sulfonic acid concentration on the reaction rate had not been determined. Therefore, in paper VI the reaction rates to TAME with the ion-exchange resin bead catalysts (A16, A35 and XE586) and a fibrous catalyst (SMOPEX-101) were measured as a function of temperature (323-353 K) with stoichiometric amount of reagents fed to a continuous stirred tank reactor.

Of the catalysts studied, A35 turned out to be the most active catalyst, especially at elevated temperatures (≥ 70°C) when the reaction rates were calculated versus catalyst mass (equation 2) or sulfonic acid concentration (equation 3) (Figures 1 a) and b)/[VI]). This must be due to hypersulfonation [40]. The next most active catalyst was A16, and the fibre catalyst showed moderate activity. Activity was surprisingly low for the surface-sulfonated XE586. Beforehand we had thought that XE586 might be very active since the active sites are located in easily accessible macropores and there should be no intraparticle diffusion limitations. Since it turned out that this was not the case, and since

the fibre catalyst showed only moderate activity, we were inclined to conclude that the *density* of the active sites is the key parameter in rendering a catalyst suitable for etherification or for other acid-catalysed reactions in organic phase, such as dimerisation of alkenes. The most interesting observation is that when the rates are calculated according to equation (4), *i.e.* when the rate is expressed in inverse proportion to the square of the sulfonic acid concentration, all catalysts showed similar activity, except for XE586, which was more active (Figure 1 c)/[VI]). This result might suggest that the etherification reaction proceeds via a *dual-site mechanism*, at least in stoichiometric conditions. However, the observed result can also be a coincidence. The observed second-order of protons can also come from the fact that different proton capacities will lead to a different swelling behaviour of the catalyst body and to a different degree of solvation of protons.

7.2 Kinetic experiments with SMOPEX-101

A fibrous catalyst had been studied in our laboratory earlier, in the etherification of C_8-alkenes, and it had been shown that no mass transfer limitations are associated with it [41,42]. It was therefore of interest to carry out a number of kinetic experiments with a fibrous catalyst in order to perform kinetic modelling and to compare the results obtained with Amberlyst 16 used as the catalyst [I,II]. The rates of TAME formation and the isomerisation of isoamylenes as a function of temperature (333-353 K), the feed MeOH/isoamylene molar ratio (0.5-2.0), as well as the splitting of TAME were measured in a batch reactor with SMOPEX-101 as the catalyst. At the temperatures studied, the initial rate of ether formation was about twice that of isomerisation when an equimolar ratio of methanol and 2M1B was used as the feed, whereas the initial rate of etherification

was about 10 times that of isomerisation when an equimolar ratio of methanol and 2M2B was used. The etherification of 2M1B was two to three times as fast as the etherification of 2M2B. The splitting of TAME with a dilution of 50 mol-% of isopentane was about four times as fast as the formation of TAME under stoichiometric conditions with a dilution of 10 mol-% of isopentane. These general trends are in line with earlier observations made with Amberlyst 16 as the catalyst [I].

The formation of *tert*-amyl alcohol from the isoamylenes and water was detected in the experiments. Because the catalyst was dry when placed into the reactor, the water needed for the formation of the *tert*-amyl alcohol must have come from the dehydration reaction of methanol. The *tert*-etherification rate of isoamylenes was 40 to 240 times that of the hydration rate of the isoamylenes to form TAOH (Table 3/[VI]). With Amberlyst 16 the rate of *tert*-etherification was 140 to 270 times that of the dehydration rate and consequent hydration rate (Table 3/[IV]). Dimerisation of isoamylenes was detected only at higher temperatures (≥ 343 K) and in the experiments where alkenes were fed in excess (MeOH/IA=0.5). The *tert*-etherification rate of the isoamylenes was 240 to 450 times that of the dimerisation of the isoamylenes to form DIA (Table 3/[VI]). The dimerisation has been observed with Amberlyst 16 only at low alcohol/alkene ratios [37].

7.2.1 Kinetic modelling

Two types of kinetic models were tested against these batch reactor experimental data with SMOPEX-101 as the catalyst. The Eley-Rideal type model [I,II] was based on the assumption that only the alcohol and ether are adsorbed on a *single* acid site of the catalyst. The Langmuir-Hinshelwood type model assumed that the reactive components

are adsorbed on *two* adjacent acid sites, but adsorption of the alcohol is dominant [II,24]. The estimated parameters for the two different kinetic models are presented in Table 7.

The smaller residual sum of squares (RSS) for the dual-site mechanism than for the single-site mechanism shows that the dual-site mechanism is more appropriate. Also, for three of the parameter values the standard error (SE %) is one or two percentage points smaller with the LH mechanism than with the ER mechanism. This is in line with our previous results with Amberlyst 16 as the catalyst [II].

Table 7. Modelling results with SMOPEX-101

Model	**Eley-Rideal**				**Langmuir-Hinshelwood**			
			95% confidence limits				95% confidence limits	
Parameter	value	SE %	lower	upper	value	SE %	lower	upper
k_1(mol/kg*s)	0.0134	8	0.0114	0.0153	0.0122	6	0.0109	0.0136
E_1(J/mol)	110051	5	98191	121910	92689	5	82755	102624
k_3(mol/kg*s)	0.0077	2	0.0074	0.0080	0.0055	2	0.0053	0.0057
E_2(J/mol)	89446	2	86267	92625	93040	1	90404	95675
k_5(mol/kg*s)	0.0092	14	0.0066	0.0117	0.0062	14	0.0045	0.0078
E_3(J/mol)	106355	10	84827	127883	116721	9	96955	136487
K_T/K_M	3.83E-07	21766006	-0.16318	0.163184				
RSS				**0.064**				**0.053**

The recalculated activation energies for the basic Langmuir-Hinshelwood type model, including the correction from diffusion with Amberlyst 16 (Table 5/[III]), are in better agreement with the activation energies obtained with the fibre catalyst (Table 7): $E_{act,1}$=81.5 kJ/mol and $E_{act,2}$=95.4 kJ/mol with A16 and $E_{act,1}$=92.7 kJ/mol and $E_{act,2}$=93.0 kJ/mol with fibre, for the etherification of 2M1B and 2M2B, respectively. The recalculated rate constants at each temperature for Amberlyst 16 [III] and rate constants for SMOPEX-101 [VI] are compared in Figure 5.

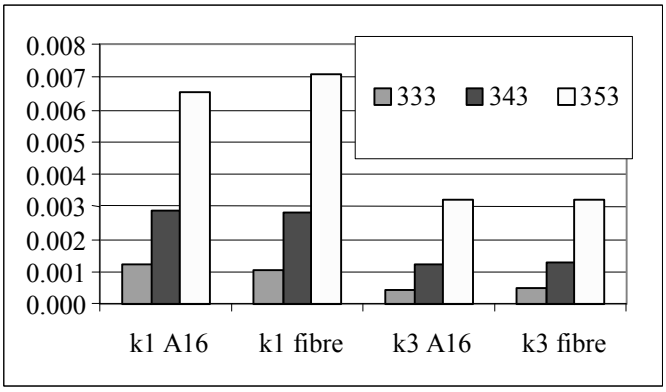

Figure 5. Comparison of the etherification rate parameters (k_1 and k_3; 1/(H^+*s)) with Amberlyst 16 [III] and SMOPEX-101 [VI] as catalyst at temperatures of 333-353 K

Figure 5 shows that the recalculated values of the etherification rate constants are quite similar for the bead catalyst and for the fibre catalyst. If mass transfer is not taken into account for the bead catalyst, the values of the rate constants are higher for the fibre catalyst than for the bead catalyst (Figure 2/[VI]). Taking into account that the recalculated rate constants for Amberlyst 16 are estimates, since the calculation of effectiveness factors was based on estimated diffusion coefficients, Figure 5 implies that mass transfer was treated rather succesfully in paper III.

8. CONCLUSIONS

The etherification reaction of isoamylenes with methanol to the fuel ether TAME on an ion-exchange resin seems to happen via a dual-site mechanism. Kinetic modelling results from the experiments with the bead catalyst (Amberlyst 16) and with the fibrous catalyst (SMOPEX-101) favoured the Langmuir-Hinshelwood type model, which was derived from a dual-site mechanism. Also, comparison of several catalysts (A35, A16, SMOPEX-101 and XE586) showed a second-order dependency on the concentration of the sulfonic acid groups.

When investigating which catalyst was the most suitable for the etherification process, the density of the active sites was found to be a key factor. Comparison of catalysts showed that the activity order was A35>A16>SMOPEX-101>XE586 when the steady-state reaction rates were calculated versus the weight or the plain acid capacity of the catalysts. Hypersulfonated catalyst, such as Amberlyst 35, is therefore highly recommended on the basis of the weight-based results.

For the ion-exchange resin bead catalyst (Amberlyst 16) a kinetic model expressed in component activities was presented for reactor design purposes. The model included relative adsorption equilibrium constants and an empirical correlation for the acceleration of isomerisation kinetics. If a basic Langmuir-Hinshelwood type model is applied for reactor design purposes, mass transfer effects should be taken into account for bead catalysts. This was noticed when comparing the kinetic modelling results for the fibrous catalyst (SMOPEX-101) and the bead catalyst (Amberlyst 16). The rate parameters of the basic model and their activation energies were higher for the fibre catalyst than for the bead catalyst. Mass transfer of the reacting components inside the pores of the bead

catalyst could be estimated in terms of the effectiveness factors calculated from experiments carried out with different bead sizes. Diffusion corrected rate constants and resulting increased values of activation energies for the bead catalyst agreed better with the values of the rate constants and their activation energies for the fibrous catalyst. However, the validity of the proposed model for bead catalyst is still restricted to amounts of methanol greater than 5 wt-% or 10 mol-%.

As a side reaction in the synthesis of TAME and TAEE, the formation of dialkyl ethers DME and DEE from methanol and ethanol, respectively, was favoured by high temperature and high alcohol concentration. At higher temperatures, dimethyl ether formed at a faster rate than diethyl ether. When the reaction was maintained in a kinetic regime, the reaction was highly selective for *tert*-etherification, since the rate of *tert*-etherification was 140 to 270 times that of dehydration. Within the experimental range studied, alcohol dehydration was best described with a model where one alcohol molecule is adsorbed and the other reacts from the liquid phase.

From the other complete kinetic models presented for TAME synthesis in the literature, models based on component activities described the etherification kinetics and reaction equilibrium better under a wider range of conditions than models based on component concentrations. Concentration-based homogeneous models described the kinetics and equilibrium only under conditions where methanol was initially in excess. One reason is that the parameters of the two concentration-based models were obtained from experiments where methanol was initially in excess. A more fundamental reason could be that the nonideality of this particular reaction system was not properly taken into account.

ABBREVIATIONS AND IUPAC NAMES

2M1B	2-methyl-1-butene
2M2B	2-methyl-2-butene
A16	Amberlyst 16
A35	Amberlyst 35
DEE	diethyl ether, ethoxyethane
DIA	diisoamylene, 2,2,3,4-tetramethylhexene
DME	dimethyl ether, methoxymethane
ER	Eley-Rideal (mechanism)
ETBE	ethyl *tert*-butyl ether, 2-ethoxy-2-methylpropane
CFRR	continuous flow recycle reactor
FCC	fluid catalytic cracking
IA	isoamylenes mixture (2M1B+2M2B)
Isobutene	2-methylpropene
LH	Langmuir-Hinshelwood (mechanism)
MeOH	methanol
MON	motor octane number
MTBE	methyl *tert*-butyl ether, 2-methoxy-2-methylpropane
PB	packed bed
RON	research octane number
RSS	residual sum of squares
Rvp	Reid vapour pressure
SE	standard error
TAEE	*tert*-amyl ethyl ether, 2-ethoxy-2-methylbutane
TAME	*tert*-amyl methyl ether, 2-methoxy-2-methylbutane

TAOH *tert*-amyl alcohol, 2-methyl-2-butanol

SYMBOLS

a_i activity of component $i = \gamma_i x_i$

E_{act} activation energy, J mol^{-1}

F_i molar flow of component i, mol s^{-1}

$\Delta_f G$ Gibbs energy of formation, J mol^{-1}

$[H^+]$ acid capacity of the catalyst, mmol g^{-1}

k rate constant, mol $kg^{-1}s^{-1}$or s^{-1}

K_i adsorption equilibrium constant of component i

K_j reaction equilibrium constant for reaction j, j = 1-3

$\dot{m}_{tot}$ total flow, kg s^{-1}

M_i molar mass of component i

r_i rate of reaction for component i, mol $kg^{-1}s^{-1}$or s^{-1}

W_{cat} catalyst mass, g

w_i weight fraction of component i

x_i molar fraction of component i

Greek letters

γ_i activity coefficient for component i

Subscripts

1b	2-methyl-1-butene
2b	2-methyl-2-butene
ETHER	etherification
ISOM	isomerisation
M	methanol
T	TAME

REFERENCES

1 J. Kivi, O. Krause, L. Rihko, *Kem. Kemi* **18** (1991) 356-359.

2 P. Lindquist, H. Järvelin, E. Tamminen, M. Koskinen, J. Aittamaa, *Proceedings of the 2nd Nordic Symposium on Reactive Separation Systems*, Helsinki University of Technology, Finland, June 1996.

3 H. L. Brockwell, P. R. Sarathy, R. Trotta, *Hydrocarbon Process*. **70** (1991) No. 9, 133-141.

4 G. R. Patton, R. O. Dunn, B. Eldridge, *HTI Quarterly* Autumn (1995) 21-27.

5 T. Kaitale, E. Merikallio, E. Rautiainen, *Proceedings of the 2nd EFOA conference*, Hotel Sheraton, Rome, October 23rd, 1987.

6 J. Aittamaa, K.I. Keskinen, *Databank of the flowsheet simulator Flowbat*, HUT, 2002.

7 *CRC Handbook of Chemistry and Physics*, 63rd ed., CRC Press: USA, 1984.

8 http://www.inchem.org/documents/icsc/icsc/eics1027.htm, October 1st, 2002.

9 California Energy Commission, Publication No: P300-98-013B, 1998.

10 http://www.efoa.org/fr/what_mtbe/supply_demand.htm, October 1st, 2002.

11 J. Tejero, M. Cunill, M. Iborra, *J. Mol. Catal*. **42** (1987) 257-268.

12 L. S. Bitar, E. A. Hazbun, W. J. Piel, *Hydrocarbon Process*. **65** (1984) No. 10, 63-66.

13 *Ullmann's Encyclopedia of Industrial Chemistry*, Wiley-VCH Verlag GmbH, Weinheim, Germany, 2002 [online]. Methyl-*tert*-butyl ether: Chapter 4. Production.

14 I. Miracca, L. Tagliabue, R. Trotta, *Chem.Eng.Sci*. **51** (1996) 2349-2358.

15 H. Subawalla, J. R. Fair, *Ind.Eng.Chem.Res*. **38** (1999) 3696-3709.

16 J. J. Jakkula, J. Ignatius, H. Järvelin, *Fuel Reformulation* (1995) No. 1, 46-54.

17 J. Gmehling, U. Onken, *Vapor-Liquid Equilibrium Data Collection*, Chemistry Data Series, Dechema: Frankfurt, 1977, Vol 1.

18 A. Fredenslund, J. Ghemling, P. Rasmussen, P. *Vapour-liquid Equilibria Using UNIFAC*, Elsevier, New York, 1977, p. 380

19 L.K. Rihko-Struckmann, J.A. Linnekoski, O.S. Pavlov, A.O.I. Krause, *J. Chem. Eng. Data* **45** (2000) 1030-1035.

20 C. Fite, M. Tejero, M. Iborra, F. Cunill, J.F. Izquierdo, *AIChE J.* **44** (1998) 2273-2279.

21 N. Oktar, K. Mürtezaogly, T. Dogu, G. Dogu, *Can. J. Chem. Eng*. **77** (1999) 406-412.

22 A. Kogelbauer, J. Reddick, D. Farcasiu, *J. Mol. Catal. A: Chemical* **103** (1995) 31-41.

23 I.P. Pavlova, D.N. Caplic, I.V. Isuk, M.E. Basner, *CNIIE - Neftechim*, Moscow,1986.

24 C. Oost, U. Hoffmann, U., *Chem. Eng. Sci*. **51** (1996) 329-340.

25 L.K. Rihko, A.O.I. Krause, *Ind. Eng. Chem. Res.* **34** (1995) 1172-1180.

26 E.G. Scheibel, *Ind.Eng.Chem*. **46** (1954) 2007.

27 A.Vignes, *I&EC Fundamentals* **5** (1966) 189-199.

28 H. Kooijman, R. Taylor, *Ind..Eng.Chem. Res.* **30** (1991) 1217-1222.

29 R. Aris, *The Mathematical Theory of Diffusion and Reaction in Permeable Catalysts*, Volume I, Clarendon Press, Oxford, 1975, p.168.

30 H.-B. Jin, F.-R. Xiao, C.-Y. Yang, Z.-M. Tong, *Shiyou Huagong Gaodeng Xuexiao Xuebao* **15** (2002) 26-32 (Abstract: CAPLUS, American Chemical Society).

31 A. Higler, R. Krishna, R. Taylor, *Ind. Eng. Chem. Res.* **39** (2000) 1596-1607.

32 K. J. Laidler, *Chemical Kinetics*, Harper & Row Publishers Inc., New York, 1987, p. 245.

33 W-S. Hwang, J-C.Wu, *J. Chin. Chem. Soc.* **41** (1994) 181-186.

34 R. L. Piccoli, H. R. Lovisi, *Ind. Eng. Chem. Res*. **34** (1995) 510-515.

35 *TRC Thermodynamic Tables*, Thermodynamics Research Center, The Texas A & M University System: College Station, Texas, Vol. V, 1986, p. 6101.

36 C. Thiel, U. Hoffmann, *Chem. Ing. Tech*. **68** (1996) 1317-1320.

37 L. K. Rihko, J. A. Linnekoski, A. O. I. Krause, *J. Chem. Eng. Data* **39** (1994) 700-704.

38 C. Thiel, K. Sundmacher, U. Hoffmann, U., *Chem. Eng. Sci*. **52** (1997) 993-1005.

39 W.-B. Su, J.-R. Chang, *Ind. Eng. Chem. Res.* **39** (2000) 4140-4147.

40 B. Corain, M. Zecca, K. Jerábek, *J. Mol.Catal*. **177** (2001) 3-20.

41 R.S. Karinen, A.O.I. Krause, K. Ekman, M. Sundell, R. Peltonen, *Stud. Surf. Sci. Catal.* **130** (2000) 3411-3416.

42 J. Lilja, J. Aumo, T. Salmi, D. Yu Murzin, P. Mäki-Arvela, M. Sundell, K. Ekman, R. Peltonen, H. Vainio, *Appl.Catal. A:General* **228** (2002) 253-267.